Band structure of core-shell semiconductor nanowires

M.-E. Pistol*
Solid State Physics, The Nanometer Structure Consortium, Lund University, P.O. Box 118, SE-221 00 Lund, Sweden

C. E. Pryor†
Optical Science and Technology Center and Department of Physics and Astronomy, University of Iowa, Iowa City, Iowa 52242, USA

(Received 21 May 2008; revised manuscript received 19 August 2008; published 23 September 2008)

We have calculated band structures for strained core-shell nanowires involving all combinations of AlN, GaN, and InN, as well as all combinations of AlP, GaP, AlAs, GaAs, InP, InAs, AlSb, GaSb, and InSb, as functions of core and shell radii. This gives 78 combinations, most of which have not been experimentally realized, and provides a quite complete overview of which interesting structures can be realized in core-shell zinc-blende III–V nanowires. Both the Γ- and the X-conduction-band minima were included in the calculations in addition to the valence-band maximum. The calculations were performed using continuum elasticity theory for the strain, eight-band strain-dependent $\boldsymbol{k}\cdot\boldsymbol{p}$ theory for the Γ-point energies, and a single-band approximation for the X-point conduction minima. All combinations of materials having type-I, type-II, and type-III (broken gap) band alignments have been identified, as well as all combinations for which one material becomes metallic due to a negative band gap. We identify structures that may support exciton crystals, excitonic superconductivity, and biomolecular detection. We have also computed the effective masses from which the confinement energy may be estimated. While graphical presentation of the results helps identify trends, all the numerical results are also available online.

DOI: 10.1103/PhysRevB.78.115319 PACS number(s): 73.22.−f, 73.21.Hb

I. INTRODUCTION

In recent years it has become possible to grow semiconductor nanowires for fundamental studies as well as for applications in transport, optics, and biology.[1,2] With some fabrication methods, such as the vapor-liquid-solid method,[3] it is possible to vary the material along the nanowire[4] and to cap the wire with a surrounding shell of a different material,[5,6] resulting in a core-shell nanowire. Different combinations of core and shell materials result in different strain and confinement effects, which have been measured in such structures.[7] With the wide choice of materials combinations available, it is extremely useful to know in advance which combinations are most promising for experimental investigation.

In most studies to date, the constituent materials have been III–V semiconductors or combinations of Si,[8] Ge, and C.[9] In III–V systems the crystal structure of the wires may be either zinc blende or wurtzite with mixtures of both structures occurring in some wires. Most wires grown by the vapor-liquid-solid method have a hexagonal cross section with the axis of the wire oriented along the [111] direction.[10] For core-shell nanowires composed of lattice-matched materials (e.g., GaAs and AlAs), the electronic structure is trivial. However, if the core and the shell materials have different bulk lattice constants, then the nanowire will be strained, which will affect the band structure.[11] Since the strain depends on the relative sizes of the core and shell regions as well, there are a large number of possible core-shell nanowire configurations, all with different electronic structure.

Figure 1 shows the different types of band alignments possible between the core and shell—type I, type II, and type III (broken gap). It is also possible for strain to induce a negative band gap in which the conduction band is below the top of the valence band. Type III and negative band-gap structures provide interesting wires in which metallic conductivity is realized without doping and in some cases the nanowires support simultaneous hole and electron conduction. Due to the confinement of electrons and holes to different regions, type-II and type-III structures are good candidates for producing exciton crystals.[12]

In this paper we consider III–V zinc-blende semiconductor nanowires oriented along [111] with hexagonal cross section (see Fig. 2). We have calculated the energies of the band edges of core-shell nanowires using all combinations of AlN,

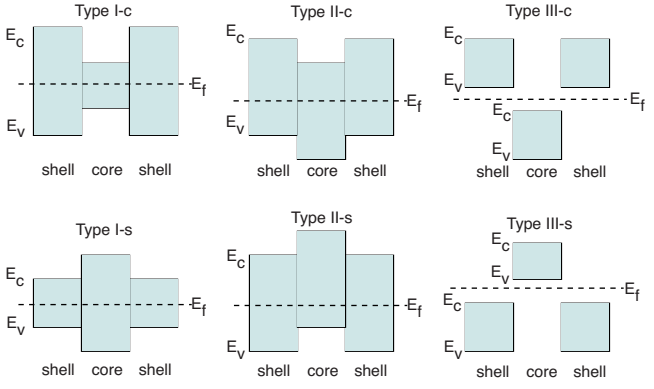

FIG. 1. (Color online) Different types of band alignments. The band gap is colored blue in the figure, E_c is the conduction-band minimum, E_v is the valence-band maximum, and E_f is the Fermi level. A type I-c structure is a normal quantum well, which can bind both electrons and holes to the core. A type II-c structure confines only electrons to the core material or holes for a type II-s structure. A type-III or broken gap structure has the valence-band maximum of one material at a higher energy than the conduction-band minimum of the other material. Electrons are transferred between materials, resulting in one material becoming metallic with electrons and the other metallic with holes.

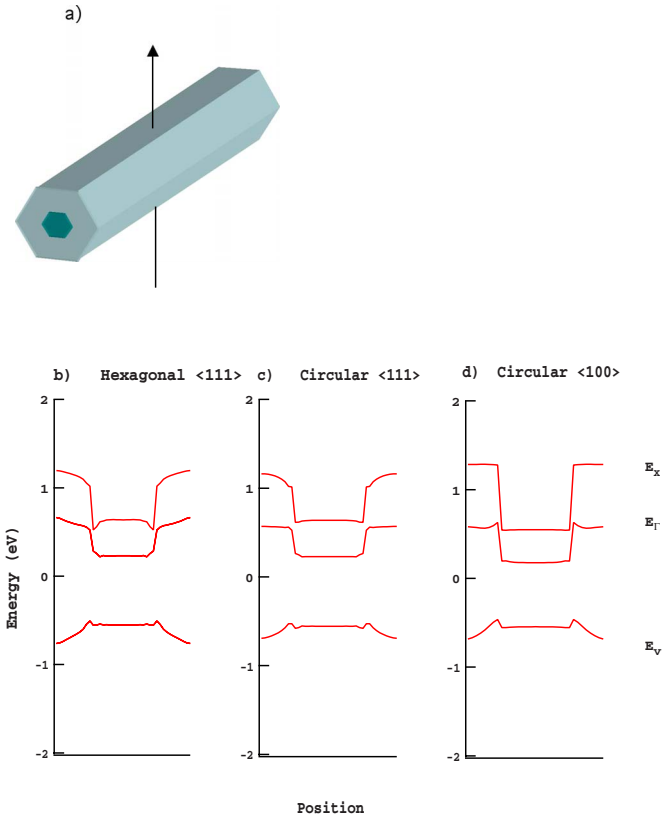

FIG. 2. (Color online) (a) Schematic of a core-shell wire with a hexagonal cross section. (b) Band edges of a hexagonal core-shell nanowire as functions of position. The arrow in (a) shows the direction along which the band edges are plotted. (c) Band edges of a circular wire oriented along the [111] direction. (d) Band edges of a circular wire oriented along the [100] direction. All wires have an InAs core and a GaAs shell, with a core radius 1/2 that of the nanowire. E_Γ is the Γ conduction-band minimum, E_X is the X conduction-band minimum, and E_V is the valence-band maximum.

GaN, and InN, as well as all combinations of AlP, GaP, InP, AlAs, GaAs, InAs, AlSb, GaSb, and InSb. We have neglected some materials, such as boron-containing compounds, as well as the wurtzite form of III–V's since the material parameters for these exotic materials are not known. Combinations of nitride and non-nitride materials were not included since the lattice mismatch is so large that we do not expect these combinations to grow in the zinc-blende structure.[13] Furthermore we expect $\boldsymbol{k}\cdot\boldsymbol{p}$ theory in conjunction with linear deformation-potential theory to be inaccurate when the lattice mismatch approaches 20%. Our treatment of nitrides has also been limited by the availability of reliable material parameters. Even for zinc-blende nitrides, it is difficult to find reliable parameters, and for most III–V compounds the parameters for the remote extrema, such as the conduction-band L point, are not known.

We also calculated the strain-dependent mean effective masses at the Γ point, which determines the transport properties. Structures with a low effective electron or hole mass and thus a possibly high mobility may be of interest for devices. The effective mass also allows one to calculate the confinement energies of the nanowire states in an effective-mass approximation (see Fig. 5). Our results provide a comprehensive overview of interesting structures that can be realized with core-shell wires, as well as provide constraints on what structures cannot be obtained.

II. METHOD

For each material combination and core and shell radii, we first computed the strain using continuum elasticity. The structure was discretized as $120\times120\times120$ cube-shaped linear finite elements and the strain energy was minimized using the conjugate gradient algorithm. It is important to note that the Hamiltonian describing the strain energy is scale invariant and, therefore, the resulting strain field applies to any structure with the same proportions regardless of overall size. Therefore the band structure depends only on the relative size of the core and shell and we plot all energies as functions of the core radius divided by the nanowire outer radius. The spatially dependent strain was used to calculate the local band edges as well as the Γ-point conduction-band effective mass at each point in the grid. The local band energies and effective masses are the values one would obtain for an electron in a bulk material with the same strain as the local value calculated for the nanowire. The Γ-point energies were calculated using strain-dependent eight-band $\boldsymbol{k}\cdot\boldsymbol{p}$ theory.[14,15] The energy of the X band was calculated in the single-band approximation,

$$E_X = \Xi_u \,\mathrm{Tr}\, e + \Xi_d k_i e_{ij} k_j, \tag{1}$$

where Ξ_u and Ξ_d are the deformation potentials, e_{ij} is the strain tensor, and k_i is a unit vector in the direction of the particular X valley being considered.

Presenting every band structure we have calculated (such as Fig. 2) is not feasible nor very useful. Instead, we have computed spatial averages of the band energies and effective masses separately over the core and shell regions for each material combination. This results in a single quantity for each geometry, which is plotted as a function of the core size, in order to compare different geometries. In Fig. 2 we show a nanowire with an InAs core and a GaAs shell, as well as the band energies within the wire. Due to the large lattice mismatch this is a highly strained system, and the band energies vary spatially due to the inhomogeneity of the strain. However, as can be seen from Fig. 2, even in such a highly strained system the spatial variation in the band energies is not very large and, hence, a spatial average of the energies in the core and shell serves as a useful measure of the band structure.

We also see in Fig. 2 that the band structure for circular wires oriented along the [111] or the [100] direction is very similar to the hexagonal wires in the core, suggesting that our results apply to circular nanowires as well. Even for the shell the differences are reasonably small.

We assumed a zinc-blende crystal structure and the wires were assumed to have a hexagonal cross section and to be oriented along the [111] direction. We expect that our results will also be useful even if the constituent materials have a wurtzite structure since the wurtzite material parameters are very close to those for zinc blende[16,17] (about 5%–10% difference) in the known cases.

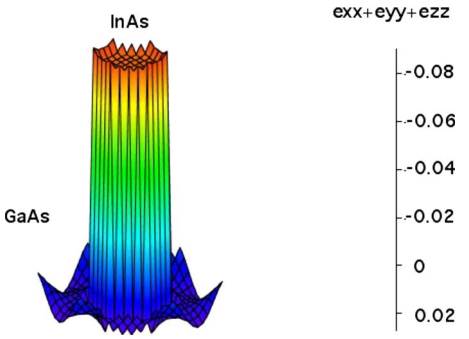

FIG. 3. (Color online) The hydrostatic strain in a hexagonal [111]-oriented InAs/GaAs core-shell nanowire. The core radius is 1/2 the outer radius of the wire. Note that the strain is quite uniform, especially in the core.

Material parameters were taken from Refs. 18 and 19, except for the X valley deformation potentials, which were taken from Refs. 20 and 21. The parameters for the nitrides, and especially those for the X valleys, are more uncertain than for the non-nitride materials since they are, in most cases, obtained from theory alone. In some unstrained materials the L-point conduction-band minimum is lower in energy than the X-point conduction-band minimum. However, under hydrostatic compression both the L and the Γ minima move to a higher energy, whereas the X minimum moves to a lower energy. As a result, in most strained materials the X- or Γ-point minimum is lowest in energy, and so we have not computed the L-valley energies. GaSb is an exception, since its L and Γ minima are so close, and GaSb should be treated with some care.

III. RESULTS AND DISCUSSION

Before examining the band structure, we first consider the strain itself. Figure 3 shows the hydrostatic strain, $e=e_{xx}+e_{yy}+e_{zz}$, on a cross section of an InAs/GaAs hexagonal wire oriented along [111]. The hydrostatic strain is quite uniform and negative in the core (i.e., compressive since bulk InAs has a larger lattice constant than GaAs) while the tensile strain of the shell is less uniform. If the GaAs shell is very thin, it looks like a quantum well grown on a material with a larger lattice constant and is consequently under tension. If the shell is infinite, however, the InAs core will be under compression and will push against the shell resulting in compressive strain in the shell at least near the core. We thus have the peculiar situation that for some shell thickness, the core is under compression while the average hydrostatic strain in the shell is zero.

We now turn to the band structures. Figure 4 shows a typical result along with the band diagram for one particular core radius extracted from it. It is interesting that the energy of the Γ conduction-band minima of both the core and the shell move together as a function of core radius. The Γ conduction-band minimum responds only to the hydrostatic part of the strain.[22] Thus if the core becomes more compressed then so does the shell. This is true regardless of whether the shell has a smaller or a larger lattice constant

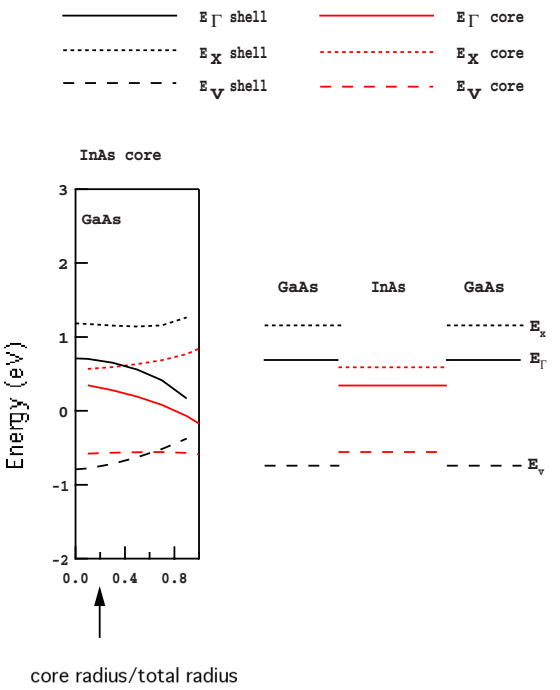

FIG. 4. (Color online) Band edges for a wire with a core of InAs and a shell of GaAs. The dashing of the lines indicates that the energy corresponds to the Γ conduction band (no dash), the X conduction band (short dash), or the valence band (long dash). The lines for the shell energies are black and the lines for the core energies are red. The example in the figure has a core radius of 0.2 of the total radius. (The radius is defined as the distance from the center of the wire along the $[01\bar{1}]$ direction.) Reading off the energies of the various bands at this core radius, we can easily construct the effective band-edge diagram of this particular core-shell wire as illustrated in the figure. We see that the InAs core acts as a quantum well with a direct band gap and that the GaAs shell is a barrier, also with a direct band gap. The bands are not flat in a real structure but the variation with position is not very large (see Fig. 2).

than the core and this is born out by the calculations. We group our results by common core materials and plot the band energies as functions of core size.

As already mentioned, since the strain is independent of the overall size of the wire, the band diagrams apply to any wire with the same proportions. However, the confinement energy will depend on the overall size. The confinement energy may be easily calculated if we assume the two-dimensional potential of the wire to be a hexagonal square well with a single effective mass throughout the structure. For different nanowire structures the barrier heights are found in the band diagrams that follow, while the effective masses in the core are shown in graphs available online.[23,24] Using these values Fig. 5 gives the confinement energy. Comparison with full eight-band calculations shows the results are accurate to within 5%–10%.

All of the results (energies, masses, and confinement energies) are also contained in text files available online.[23,24]

A. Nitride cores

We first consider nanowires with nitride cores shown in Fig. 6. Bulk AlN has an indirect gap of about 4.9 eV. A shell

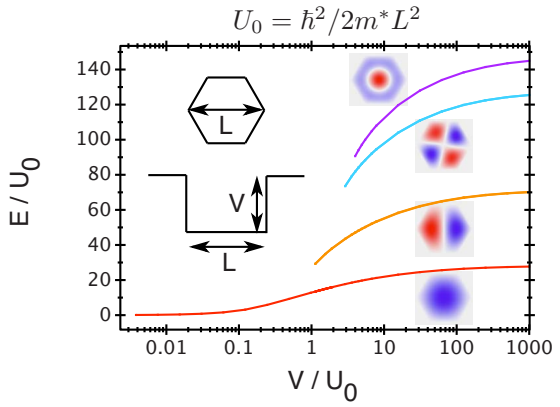

FIG. 5. (Color online) The four lowest confinement energies of a particle in a hexagonal wire as functions of the barrier height V. Quantities are in units of the characteristic energy $U_0=\hbar^2/2m^*L^2$, where L is the diameter indicated in the figure and m^* is the effective mass. For $m^*=m_e$ and $L=1$ nm, we have $U_0=38.1$ meV. Plots of the corresponding wave functions are given in the insets. For small V there is only one bound state. The insets show cross sections of the wave functions.

of GaN will form a type-I quantum well for all radii as shown in Fig. 6. Due to the small lattice mismatch between AlN and GaN, there are only small strain shifts as the core radius is varied. A shell of InN will also form a type-I quantum well. For this material combination there is a substantial difference in lattice constant and the core radius is an important parameter. If the shell is thin then the band gap of InN will be almost zero. Due to the uncertainty in the materials parameters, InN could in fact have a negative band gap and be a metal when grown as a thin shell on AlN. Bulk GaN has a direct gap of about 3.3 eV and will form a type-I quantum well when capped with a shell of AlN. A shell of InN on a core of GaN will form a type-I quantum well for almost all radii. For a very small core radius the valence-band maxima of InN and GaN will have the same energy. Bulk InN has a direct band gap of about 0.8 eV. InN will form a type-I quantum well in AlN unless the shell is very thin, in which case a type-II structure is formed with holes in the AlN and electrons in the InN. A similar phenomenon occurs for a GaN shell on an InN core.

B. AlP core

The results for nanowires with AlP cores are shown in Fig. 7. AlP has an indirect gap of about 2.5 eV and is usually thought of as a barrier material, however, AlAs and AlSb shells both form conduction-band barriers when surrounding AlP. Shells of GaP are essentially lattice matched to AlP and the band offset is type II. That is, the conduction-band minimum of AlP is below the conduction-band minimum of GaP and the valence-band maximum of AlP is below the valence-band maximum of GaP. A plot of the band edges is shown in Fig. 8, showing that photoexcited charge carriers will separate electrons to the core and holes to the shell.

We expect long-lived excitons in this system for two reasons: the indirect character of the conduction band and the spatial separation of the electrons and the holes. This is an ideal situation for an exciton crystal predicted by Ivanov and Haug.[12] The separation of charges causes the excitons to re-

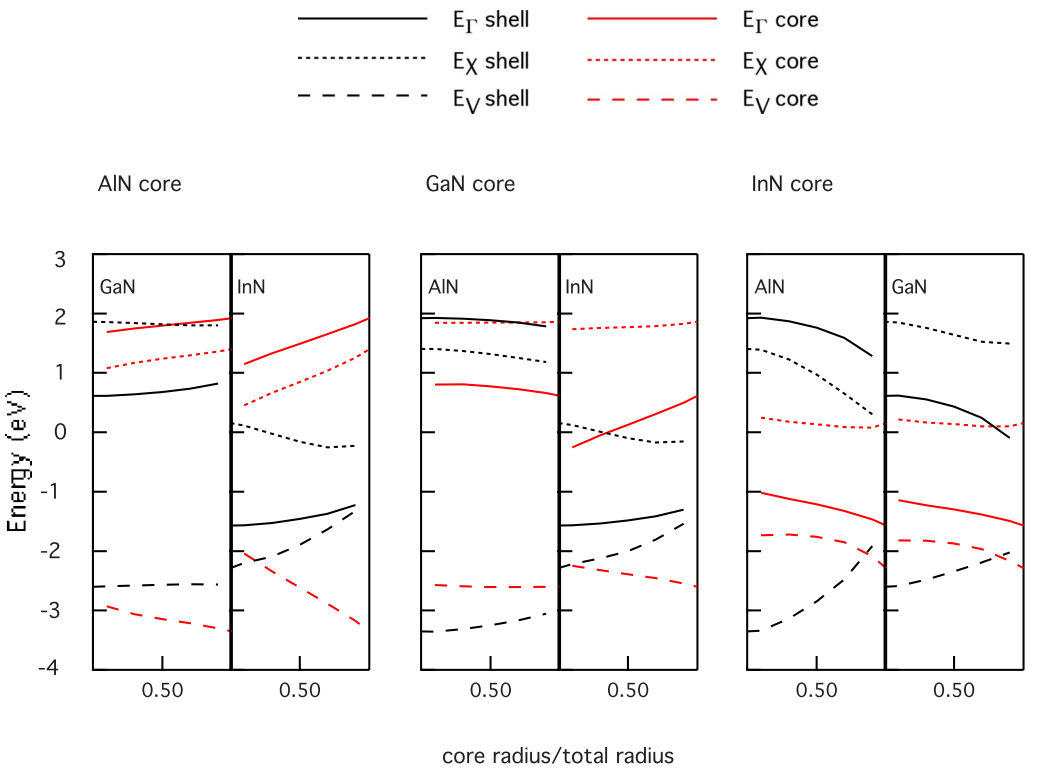

FIG. 6. (Color online) Band edges of core-shell wires with nitride cores and different nitride shells (indicated) as functions of core radius.

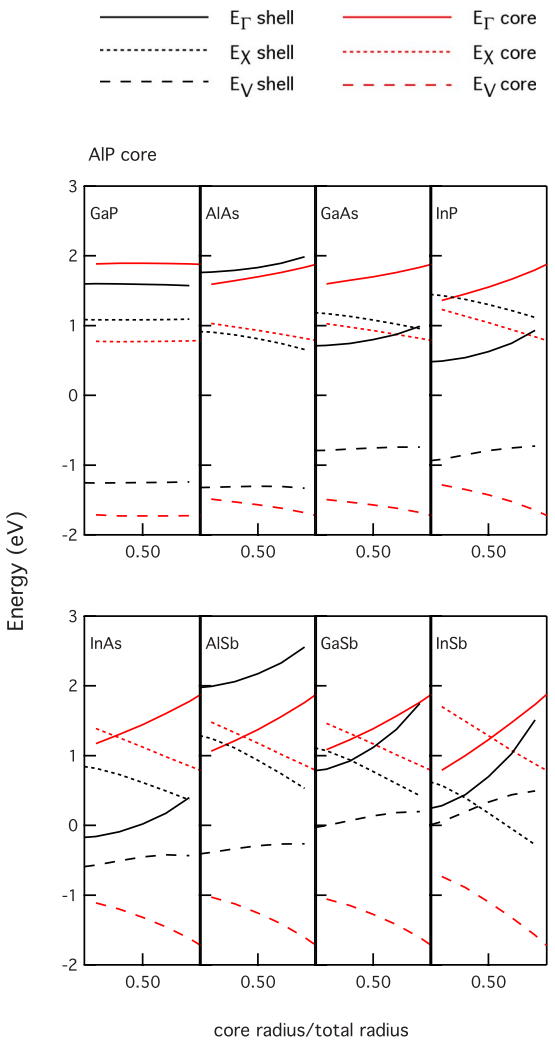

FIG. 7. (Color online) Band edges of core-shell wires with a core of AlP and different (indicated) shells as functions of core radius.

pel each other. In a finite wire with the proper exciton density, the excitons will tend to form a correlated state with excitons lying side by side in a row, unable to change places with each other, as illustrated in Fig. 8. A high melting point for this crystal of about 50 K has been predicted.

Shells of AlAs, GaAs, InP, InAs, AlSb, and GaSb have a positive band gap for all thicknesses, whereas InSb attains a negative band gap when grown on a thick AlP core. The case of InSb is especially interesting (Fig. 9). The shell is metallic, thus forming an epitaxial metal-semiconductor system, which is difficult to obtain using conventional metals.

The offset between the Fermi level of the metal and the semiconductor band edges in these epitaxial metal-semiconductor systems should be very reproducible and of higher quality than in a normal Schottky barrier or Ohmic contact. We propose that such systems could be used for contacting wires used for electronic and optical applications. The contact to the external world can be done using a normal metal contacting the epitaxial metal. This removes the fluctuations usually present in normal-metal semiconductor junctions[25] from the active region of a device based on wires.

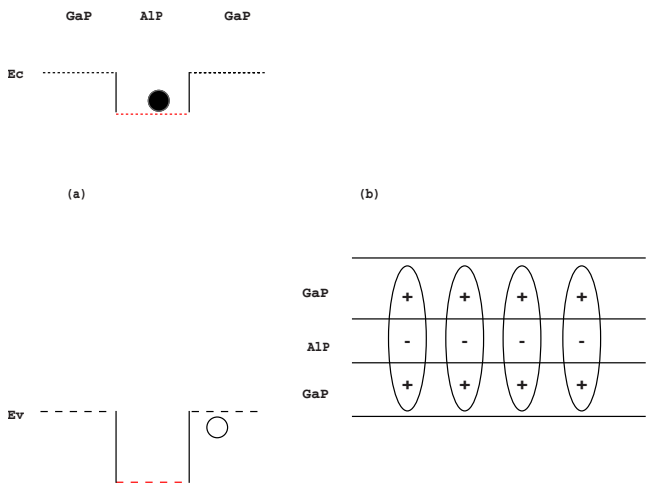

FIG. 8. (Color online) (a) Band edges of a wire having an AlP core and a GaP shell. Photoexcited charge carriers will separate electrons to the core and holes to the shell. (b) Excitons will repel each other due to the separation of charges and may form an exciton crystal, in which the excitons lie in a row and cannot easily pass each other. Since the conduction-band minima are indirect, the excitons will be long lived.

In addition, the metallic shell will shield the core from external electric fields with potential application for devices operating under adverse electrical environments. A thin core of AlP in a shell of InSb has a direct band gap in contrast to bulk AlP, which has an indirect gap.

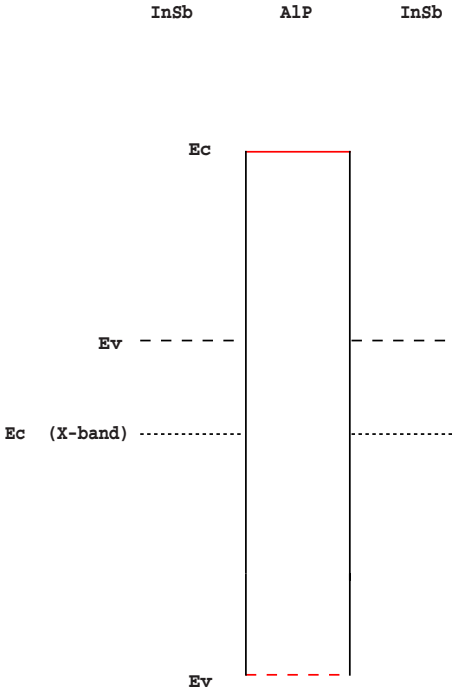

FIG. 9. (Color online) (a) Band edges of a wire having an AlP core and an InSb shell. The valence-band maximum of the shell has a higher energy than the conduction-band minimum. Consequently the shell will be metallic, having a Fermi level in the band gap of the AlP core.

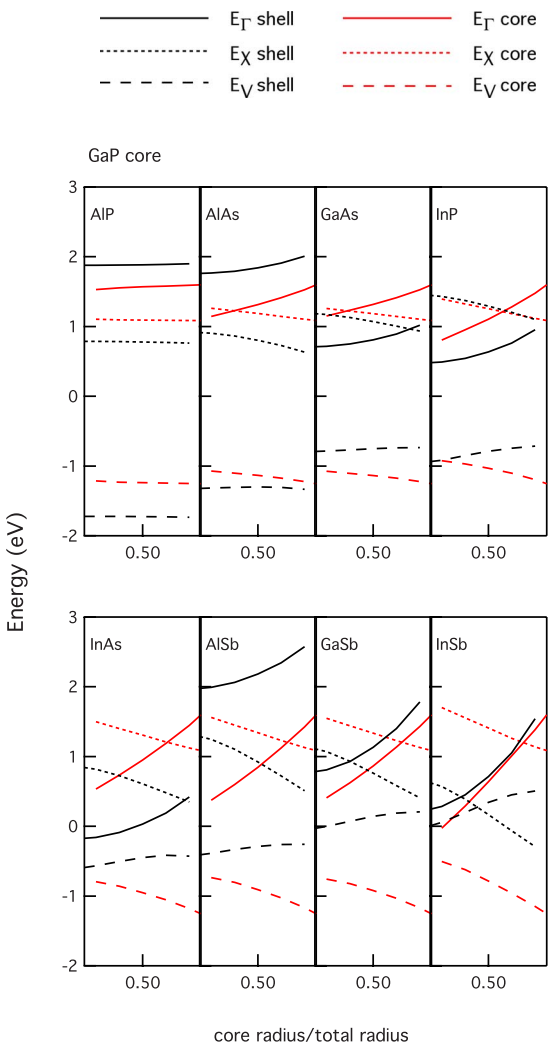

FIG. 10. (Color online) Band edges of core-shell wires with a core of GaP and different (indicated) shells as functions of core radius.

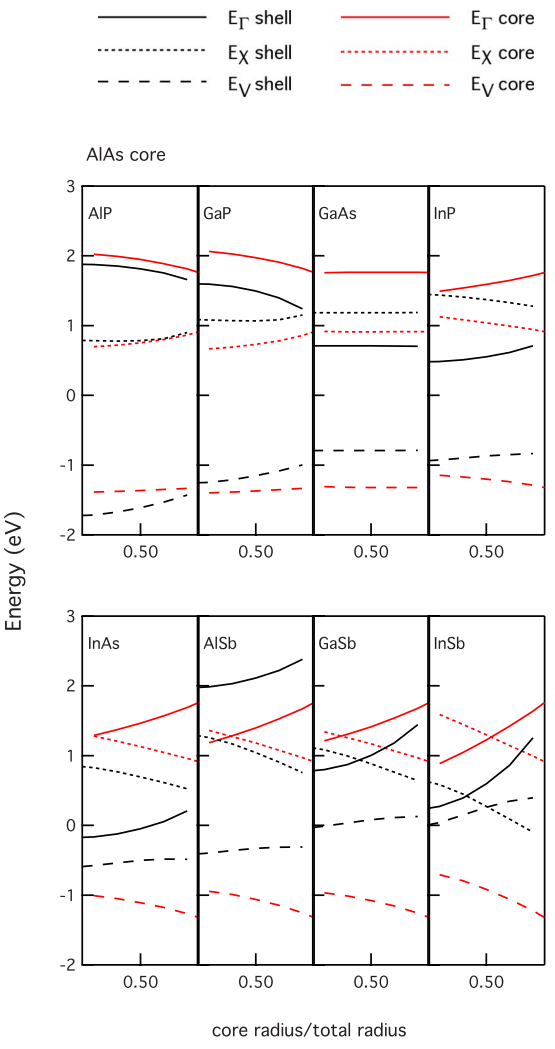

FIG. 11. (Color online) Band edges of core-shell wires with a core of AlAs and different (indicated) shells as functions of core radius.

C. GaP core

The band edges for nanowires with GaP cores are shown in Fig. 10. A shell of AlP will form a type-II structure confining electrons to the shell and holes to the core. This is also a possible system for investigations of an exciton crystal as shown in Fig. 8. A negative aspect is that AlP is sensitive to water and the inverted structure is likely more promising for experiments. A shell of AlAs will also form a type-II structure with electrons confined to the shell and holes to the core. The GaP core will have a direct band gap for the thinnest cores but will otherwise have an indirect band gap. A shell of GaAs will form a type-I well and so will a shell of InP. For a shell of InP there will be a transition of the band gap of GaP from direct to indirect at a core radius of about 0.7. A shell of InAs will form a type-I quantum well. Both AlSb and GaSb will go from a type-II structure with electrons confined in the core and holes in the shell to a type-I structure (with an indirect gap) when the radius of the core increases. A shell of InSb will—for small cores—be a broken gap (type III). The valence band of InSb will donate electrons to the core of GaP, leading to a metallic system in which both electrons and holes contribute to the conductivity. The charge carriers are separated however and this metallic wire is thus somewhat different from the metals occurring when negative gaps are present in the wire as illustrated in Fig. 9. When the core is larger, then the band edges of InSb will be in the gap of GaP. However the InSb shell will have a negative band gap and will thus still be metallic. This is an especially rich system for experimental investigation.

D. AlAs core

The band edges for nanowires with AlAs cores are shown in Fig. 11. AlAs with a shell of AlP will be a type-I quantum well with a very small offset in the conduction band. A shell of GaP will form a type-II structure with the core confining electrons and the shell confining holes. GaAs is very closely lattice matched to AlAs (as evidenced by the lack of dependence on core size) and will form a type-I quantum well. A shell of InP behaves very similarly to a shell of GaAs and is a type-I quantum well and the same is true for a shell of

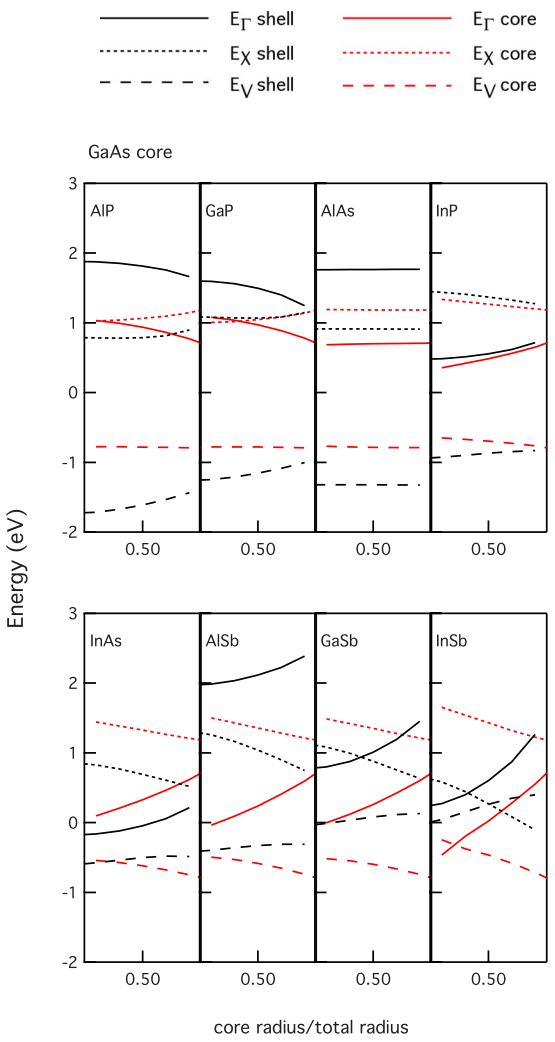

FIG. 12. (Color online) Band edges of core-shell wires with a core of GaAs and different (indicated) shells as functions of core radius.

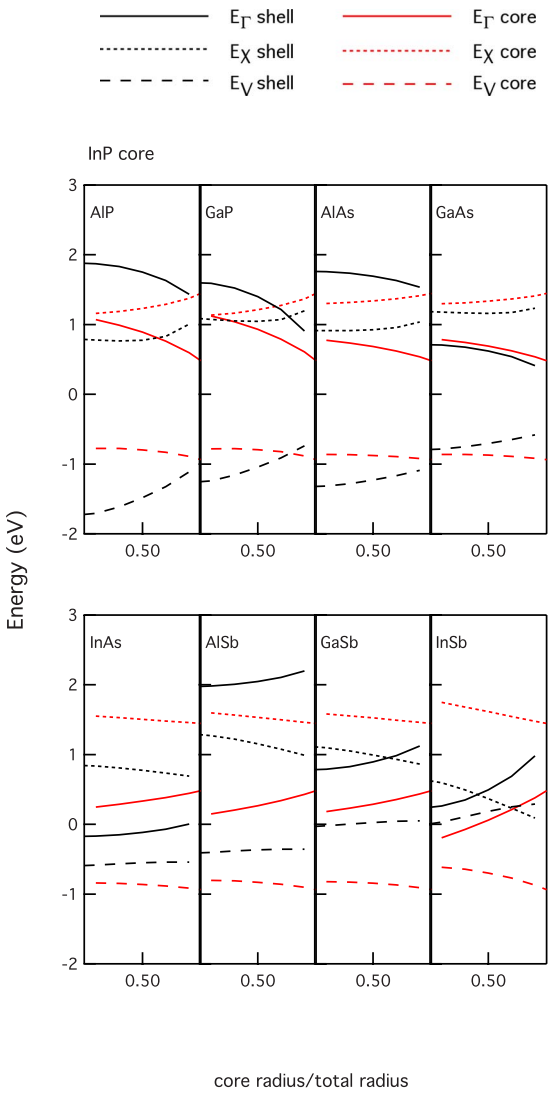

FIG. 13. (Color online) Band edges of core-shell wires with a core of InP and different (indicated) shells as functions of core radius.

InAs. A very thick shell of AlSb forms a weakly type-II structure with the core attracting electrons and the shell holes. For thinner shells of AlSb we have a type-I structure with the shell attracting the charge carriers. A shell of GaSb will form a type-I quantum well. However there is a transition from a direct band gap to an indirect band gap as the core radius increases. A shell of InSb will initially be a direct-gap type-I quantum well, then an indirect-gap type-I quantum well, and finally have a negative band gap as the core radius increases.

E. GaAs core

The band edges for nanowires with GaAs cores are shown in Fig. 12. GaAs is the most important III–V semiconductor and has received considerable attention as a wire material. A thick shell of AlP forms a type-II structure with the shell attracting electrons and the core attracting holes. When the shell is thin the GaAs core forms a type-I quantum well. A core of GaAs is a type-I quantum well when a shell of GaP or AlAs is grown. AlAs is nearly lattice matched to GaAs so there are only weak strain effects. A core of GaAs is also a type-I quantum well in a shell of InP although the band offset in the conduction band is very small. A shell of InAs is a type-I quantum well, whereas shells of AlSb and GaSb are both type-II quantum wells with electrons confined to the core and holes to the shell. A thick shell of InSb forces a GaAs core to have a negative band gap and become metallic. A thinner shell of InSb forms a type-III structure with the added twist of a negative band gap for the InSb. A very thin InSb shell has a negative band gap, where the band edges are within the band gap of the GaAs. As usual InSb forms very interesting structures.

F. InP core

The band edges for nanowires with InP cores are shown in Fig. 13. An AlP shell goes from a type-II structure to a type-I structure as the radius of the core increases with holes confined to the InP core. With a GaP shell, an InP core forms a

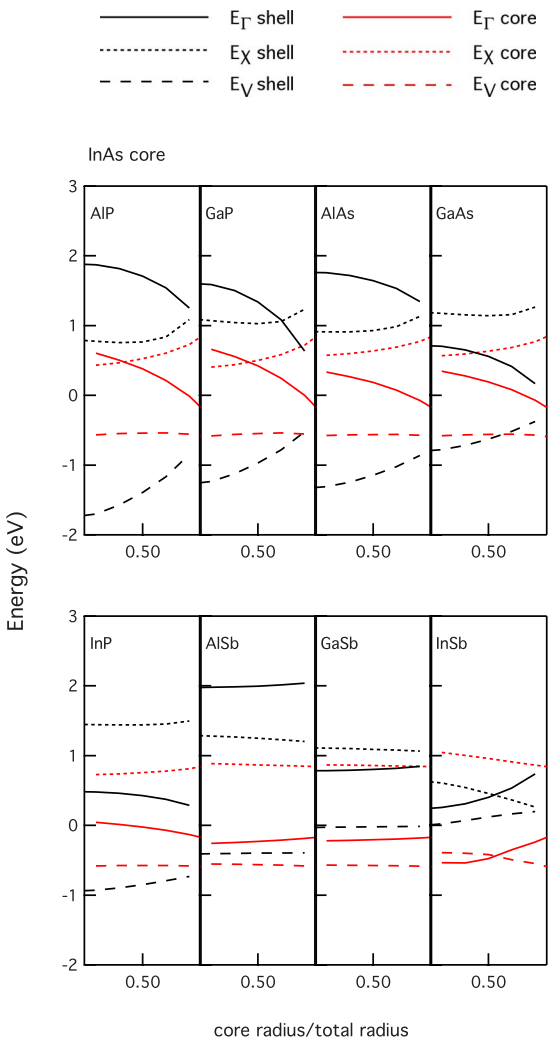

FIG. 14. (Color online) Band edges of core-shell wires with a core of InAs and different (indicated) shells as functions of core radius.

type-I structure unless the shell is very thick or very thin. In these cases the structure is weakly type II. A core of InP is a normal type-I wire if surrounded by a shell of AlAs, but a GaAs shell forms a type-I quantum well in the shell. A shell of InAs forms a type-I quantum well, whereas a shell of AlSb is type II with holes confined to the shell and electrons to the core. The same is true if the shell is GaSb. A thick shell of InSb forms a broken gap structure, and the shell donates electrons to the conduction band of the core, giving a metallic system with electron conduction in the core and hole conduction in the shell. If the InSb shell is thin, it will obtain a negative gap and be metallic, which will give rise to interesting plasmonic effects.[26] The InP will remain semiconducting though.

G. InAs core

The band edges for nanowires with InAs cores are shown in Fig. 14. InAs is an interesting material for devices requiring small band gaps such as infrared detectors. However, strain can increase the 0.4 eV band gap substantially. A core of InAs capped with AlP is highly strained. The InAs core forms a type-I structure, which is indirect for thick AlP shells but otherwise direct. The same behavior is seen when the shell is GaP and AlAs with the exception that for AlAs, there is no indirect-direct transition in the core. If the shell is GaAs, we initially have a type-I structure for small InAs cores, which becomes a type-II structure confining holes in the shell for thick InAs cores. A shell of InP forms a barrier for all thicknesses. AlSb forms a type-II structure with the core forming a well for electrons. A shell of GaSb forms a type-III structure with the GaSb valence band donating electrons to the conduction band of InAs. We thus have a metallic structure. Transport studies of such wires should be interesting since the current will be due to both electrons and holes, making it an ideal system for the study of Coulomb drag effects.[27] A small InAs core in an InSb shell has a negative band gap. A shell of InSb forms a type-III structure with the InAs core donating holes to the InSb shell. We have here a system that should be tested for excitonic superconductivity.[28] The electrons in the core of the wire may cause an attractive interaction between the holes in the shell, allowing Cooper pairs to form. The mechanism for pairing can also be viewed as electron-mediated pairing instead of exciton-mediated pairing.

H. AlSb core

The band edges for nanowires with AlSb cores are shown in Fig. 15. A core of AlSb in a shell of AlP is a marginal type-I structure where the conduction bands of the core and shell are almost degenerate for all core radii. A core of AlSb in a shell of GaP is a type-I quantum well for small radii of the core but there is a transition to a type-II structure, with electrons attracted to the shell and holes to the core, for larger core radii. The case of a shell of AlAs is very similar to the case with a shell of AlP such that the conduction-band offset is almost zero for all core radii. AlSb in a shell of GaAs, InP, or InAs forms a type-II structure with holes attracted to the core and electrons to the shell. A shell of GaSb or InSb forms a type-I quantum well. A shell of InSb has a transition from a direct gap to an indirect gap with increasing AlSb-core radius.

I. GaSb core

The band edges for nanowires with GaSb cores are shown in Fig. 16. A core of GaSb in a shell of AlP is a type-I quantum well, but only weakly so, due to a very small conduction-band offset. For a shell of GaP we have a transition from a type-I structure to a type-II structure with increasing core radius. A shell of AlAs gives a type-I quantum well with the core attracting both electrons and holes. With a shell of GaAs we have a type-II structure again with electrons attracted to the shell and holes to the core. The same situation occurs for shells of InP. A shell of InAs however forms a type-III structure with the GaSb core donating electrons to the conduction band of InAs. A GaSb core in a shell of AlSb forms a type-I quantum well. If the shell is InSb, we have a very complex behavior with two transitions between type-I and type-II structures as functions of core radius.

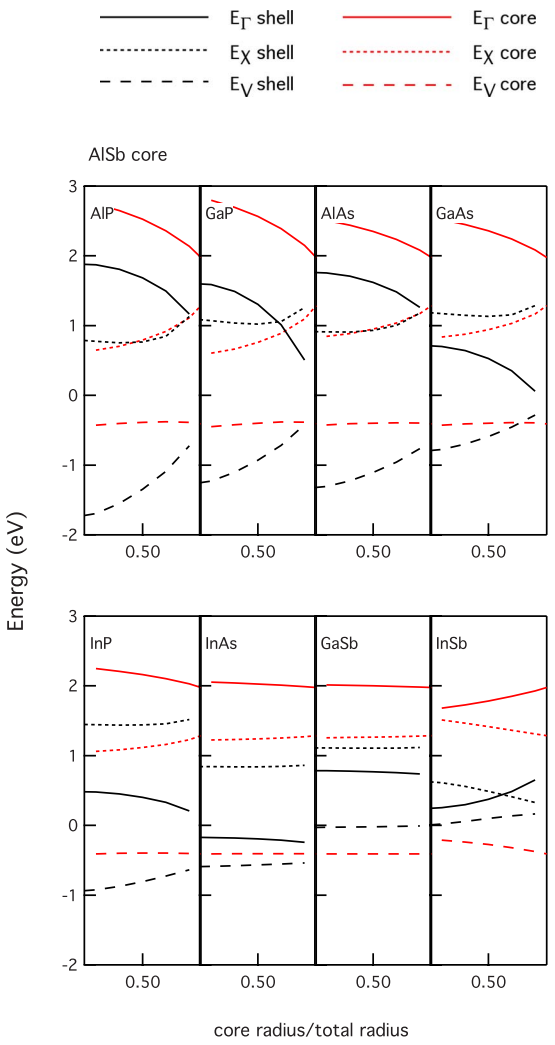

FIG. 15. (Color online) Band edges of core-shell wires with a core of AlSb and different (indicated) shells as functions of core radius.

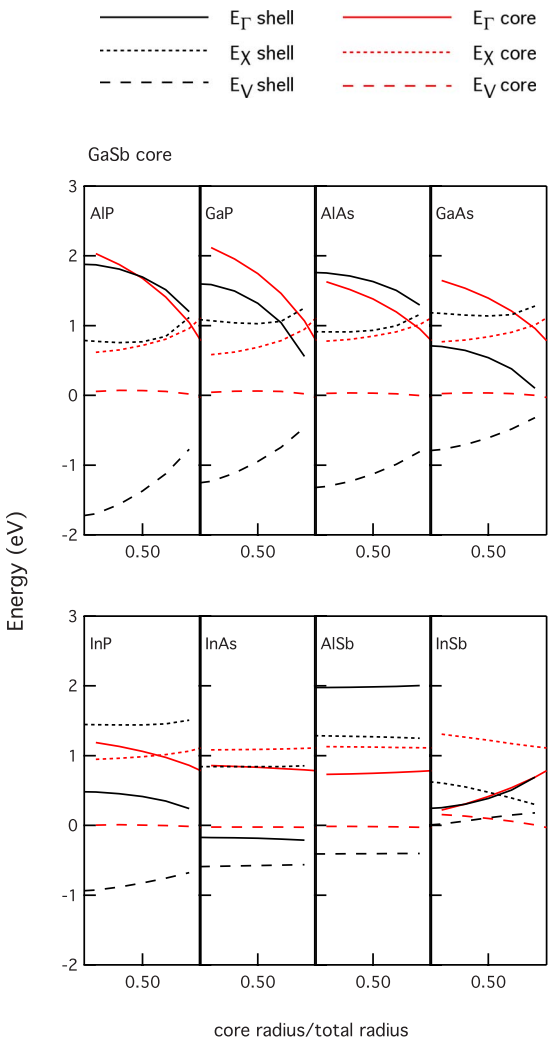

FIG. 16. (Color online) Band edges of core-shell wires with a core of GaSb and different (indicated) shells as functions of core radius.

J. InSb core

The band edges for nanowires with InSb cores are shown in Fig. 17. A core of InSb in a shell of AlP has a negative band gap for not too large core radii and is thus metallic. The shell is semiconducting though. At large core radii the band gap becomes positive and the InSb core forms a type-I quantum well. Also for shells of GaP, AlAs and GaAs the InSb core is metallic with a negative band gap if the core radius is sufficiently small. If the shell is InP, then the InSb core forms a type-I quantum well with a very small band gap for small core radii. For larger radii the structure becomes type III with the core donating electrons to the shell. A shell of InAs forms a type-III structure for small core radii. The InAs shell attains a negative band gap and becomes metallic for large core radii. A core of InSb is a type-I quantum well if the shell is AlSb and there is a transition from an indirect band gap to a direct band gap in the core with an increasing core radius. If the shell is GaSb we have a complex behavior with a transition from InSb being a type-I quantum well to GaSb being the type-I quantum well.

IV. APPLICATIONS IN PHYSICS AND TECHNOLOGY

From this exhaustive set of band diagrams we identify a few structures with especially interesting physical properties. Tables I and II summarize the band alignments in the structures shown in Figs. 6–17. The GaP/AlP system with GaP as the core and AlP as the shell has long-lived excitons that repel each other and should be a candidate for studies of exciton crystals in wires. The inverse system AlP/GaP is probably a better candidate in practical experiments since the Al-containing compound is in the core. It is not likely that a shell of AlP will survive long in a humid atmosphere. There are a few other type-II systems that can also be investigated (see Table I) but the GaP/AlP system has the advantage of emitting in a very suitable range for spectroscopy, i.e., with an energy of about 2 eV, which perfectly matches CCD detectors. Such wires may also form excitonic insulators since the charge carriers pair forming neutral excitons. In this case, the excitons would dissociate beyond a certain applied voltage or temperature, allowing a current to then flow. However for sufficiently low temperature, a one-dimensional exciton crystal would form[12] (see Fig. 8).

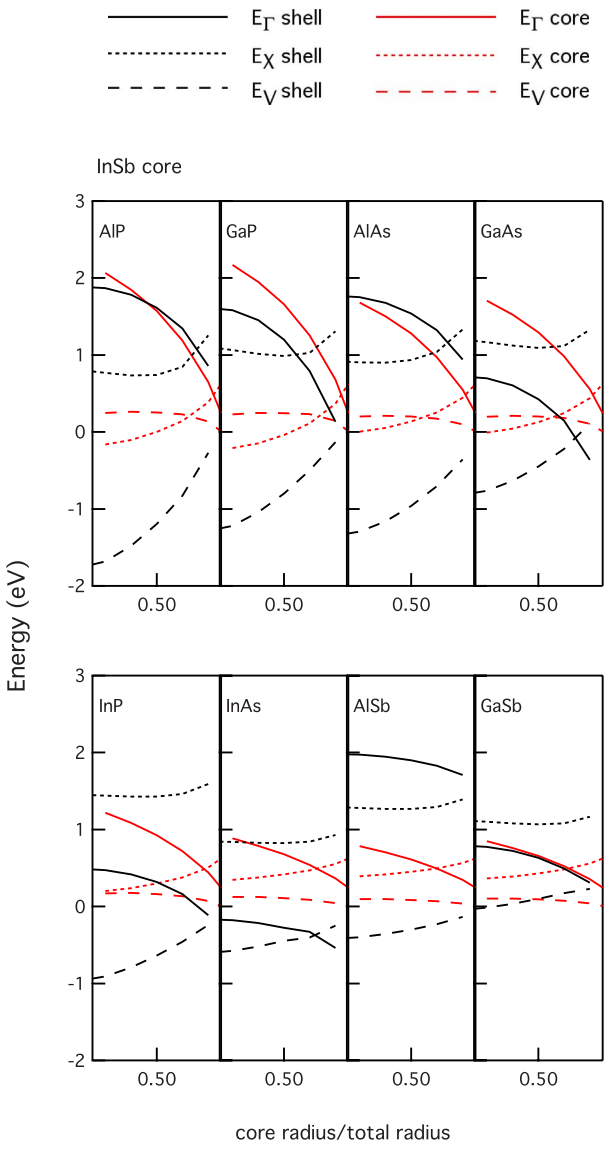

FIG. 17. (Color online) Band edges of core-shell wires with a core of InSb and different (indicated) shells as functions of core radius.

TABLE II. A table of the band alignments in different nitride core-shell systems. The notation is the same as in Table I.

	Shell material		
Core material	AlN	GaN	InN
AlN		I-s	I-s
GaN	I-c		I-s
InN	I-c	I-c	

There are several wire systems having a semiconducting core and a metallic shell due to a negative band gap of the shell. Two such systems are the GaP/InSb and GaAs/InSb, which would have epitaxial metal-semiconductor junctions allowing precise measurements of Schottky barrier heights, and the possibility of contacting wires by ordinary metals. GaAs/InSb forms an inverse system with a metallic core surrounded by a semiconductor. In this case the shell will shield the core from the surroundings, acting as an epitaxial cladding, which may be of technical use. Since metallic wires can be made with a finite length, these are good systems in which plasmonic effects can be studied.[29] Wires having metallic segments, which are situated some distance apart, will allow precise studies of the coupling of plasmons. Furthermore the metallic segments will enhance Raman scattering from the semiconductors, analogous to surface and tip-enhanced Raman scattering[26] as illustrated in Fig. 18. In fact, it may be possible to use wires that are partially metallic to detect biomolecules, where the Raman signal is measured. The wire is then coated with suitable molecules that bind the target molecule for selective detectors.

Another phenomenon to which semiconductor/metallic core-shell nanowires are well suited is excitonic superconductivity.[28] In such a superconductor, the electrons from a metal tunnel into the semiconductor, where they experience a pairing interaction via virtual excitons. This mechanism was first proposed for semiconductor/metal systems but has not been experimentally realized. Because the electrons must tunnel into the semiconductor, the pairing is sensitive to the quality of the metal/semiconductor junction.

TABLE I. Band alignments in different core-shell systems, indicating the type (I, II, or III) followed by a letter indicating whether the core (c) or shell (s) has a lower conduction band. For metallic materials, c or s indicates whether the core or shell is metallic.

	Shell material								
Core material	AlP	GaP	AlAs	GaAs	InP	InAs	AlSb	GaSb	InSb
AlP		II-c	I-s	I-s, II-c	I-s, II-c	I-s	II-c, I-s	I-s	I-s, metallic-s
GaP	II-s		II-s	I-s	I-s	I-s	II-c, I-s	II-c, I-s	III-c, metallic-s
AlAs	I-c	II-c		I-s	I-s	I-s	I-s	I-s	I-s, metallic-s
GaAs	II-s, I-c	I-c	I-c		I-c	I-s	II-c	II-c	III-c, metallic-s
InP	II-s, I-c	I-c	I-c	I-s		I-s	II-c	II-c	III-c, metallic-s
InAs	I-c	I-c	I-c	I-c, II-c	I-c		II-c	III-c	Metallic-c, III-c
AlSb	I-c	I-c, II-s	I-c	II-s	II-s	II-s		I-s	I-s
GaSb	I-c	I-c, II-s	I-c	II-s	II-s	III-s	I-c		I-c, I-s
InSb	Metallic-c, I-c	Metallic-c	Metallic-c, I-c	Metallic-c, metallic-s	I-c, III-s	III-s, metallic-s	I-c	I-c, I-s	

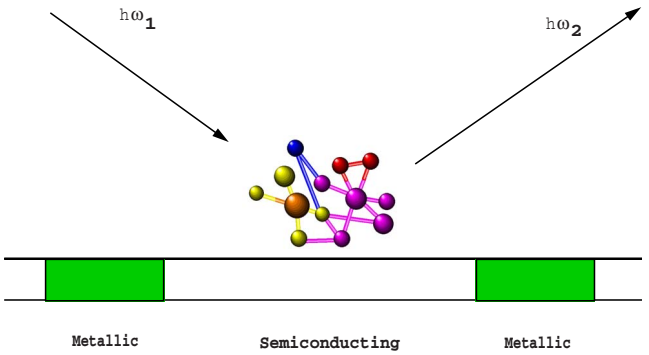

FIG. 18. (Color online) Illustration of a semiconducting wire containing two metallic segments, which enhance the Raman scattering from a molecule.

Core-shell nanowires are ideal since they will have well-formed epitaxial structure. Excitonic superconductivity also depends on the semiconductor having a resonant frequency tuned to give the maximal pairing interaction. This is somewhat difficult to engineer for a metal deposited on a semiconductor substrate. In a nanowire system, however, the core size can be chosen to tune the strain-induced properties of the semiconductor region.

V. EFFECTIVE MASSES

The Γ-point effective masses for the different quantum wires are given in additional figures available online[23] as well as in a website.[24] The effective masses for electrons in the X band are not dependent on the strain in our model and are thus not plotted. We give here one example of a mass figure (Fig. 19), showing the masses for an InP core with different shells. Due to its strain dependence, the effective mass may be varied considerably by the choice of materials and core radius. The masses for both electrons and holes generally increase when the band gap increases as they do for bulk materials. There are some exceptions to this rule particularly in the valence band. Due to the lifting of the valence-band degeneracy by shear strain, some systems have large shifts in the hole effective masses for even very thin shells or cores. In Fig. 19 it can be seen that both the electron and hole masses in the InP core can change by a factor of four depending on the thickness of an InSb shell. The normally very low effective masses in InSb can be increased considerably by growth on a thick core of InP. As another example, a GaP core in an InSb shell has an electron effective mass ranging from 0.015 to 0.1 m_e depending on core radius. The hole effective mass of InN can be changed from about 0.01 to about 0.2 m_e when grown as a shell on AlN or GaN. Also, some semiconductors with a quite large bulk electron effective mass obtain a very small effective masses in wires. For example, an InP shell grown on InSb has an electron effective mass of 0.01 m_e compared to a bulk value of about 0.08 m_e. The notion of effective masses is quite useless and ill defined when we have a negative band gap and, in these cases, we recommend that they are not used.

VI. SUMMARY

We have computed the gross electronic structure of most combinations of III–V semiconductors when they form core-shell wires. This allows the identification of a large set of structures that are of physical interest such as intrinsically metallic wires and wires having very small or very large band gaps.

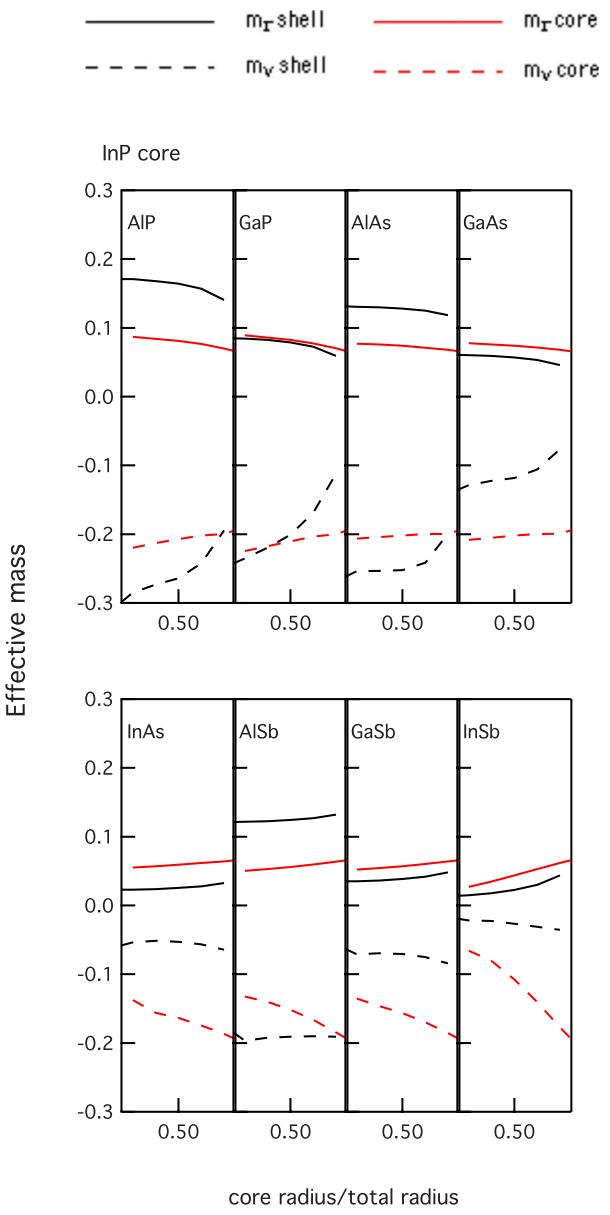

FIG. 19. (Color online) Effective masses of core-shell wires with a core of InP and different (indicated) shells as functions of core radius.

ACKNOWLEDGMENTS

We acknowledge F. Capasso for interesting discussions as well as for pointing out the possibility of excitonic superconductivity. We also thank U. Håkansson, S. Gray, and J. Trägårdh for a critical reading of the manuscript. This work was performed within the nanometer structure consortium in Lund and supported by the Swedish Foundation for Strategic Research (SSF) and the Swedish Research Council (VR). C.E.P. acknowledges support from an NSF NIRT.

*mats-erik.pistol@ftf.lth.se
†craig-pryor@uiowa.edu

[1] D. Appell, Nature (London) **419**, 553 (2002).
[2] L. J. Lauhon, M. S. Gudiksen, and C. M. Lieber, Philos. Trans. R. Soc. London **362**, 1247 (2004).
[3] R. S. Wagner and W. C. Ellis, Appl. Phys. Lett. **4**, 89 (1964).
[4] M. T. Björk, B. J. Ohlsson, T. Sass, A. I. Persson, C. Thelander, M. H. Magnusson, K. Deppert, L. R. Wallenberg, and L. Samuelson, Appl. Phys. Lett. **80**, 1058 (2002).
[5] N. Sköld, L. S. Karlsson, M. W. Larsson, M.-E. Pistol, W. Seifert, J. Trägårdh, and L. Samuelson, Nano Lett. **5**, 1943 (2005).
[6] Z. Zanolli, L.-E. Fröberg, M. T. Björk, M.-E. Pistol, and L. Samuelson, Thin Solid Films **515**, 793 (2006).
[7] Z. Zanolli, M.-E. Pistol, L.-E. Fröberg, and L. Samuelson, J. Phys.: Condens. Matter **19**, 295219 (2007).
[8] Y. Wu, R. Fan, and P. Yang, Nano Lett. **2**, 83 (2002).
[9] L. V. Radushkevich and V. M. Lukianovich, J. Phys. Chem. **26**, 88 (1952) (in Russian).
[10] S. C. Lee, L. R. Dawson, S. R. Brueck, and Y.-B. Jiang, J. Appl. Phys. **98**, 114312 (2005).
[11] C. Pryor and M.-E. Pistol, Phys. Rev. B **72**, 205311 (2005).
[12] A. L. Ivanov and H. Haug, Phys. Rev. Lett. **71**, 3182 (1993).
[13] S. B. Zhang and M. L. Cohen, Phys. Rev. B **35**, 7604 (1987).
[14] T. B. Bahder, Phys. Rev. B **41**, 11992 (1990).
[15] C. Pryor, Phys. Rev. B **57**, 7190 (1998).
[16] A. Mishra *et al.*, Appl. Phys. Lett. **91**, 263104 (2007).
[17] P. Rinke, M. Scheffler, A. Qteish, M. Winkelnkemper, D. Bimberg, and J. Neugebauer, Appl. Phys. Lett. **89**, 161919 (2006).
[18] I. Vurgaftman, J. R. Meyer, and L. R. Ram-Mohan, J. Appl. Phys. **89**, 5815 (2001).
[19] I. Vurgaftman and J. R. Meyer, J. Appl. Phys. **94**, 3675 (2003).
[20] M. C. Muños and G. Armelles, Phys. Rev. B **48**, 2839 (1993).
[21] W. J. Fan, M. F. Li, T. C. Chong, and J. B. Xia, J. Appl. Phys. **79**, 188 (1996).
[22] J. Singh, *Physics of Semiconductors and their Heterostructures* (McGraw-Hill, New York, 1993).
[23] See EPAPS Document No. E-PRBMDO-78-086835 for numerical values of band energies, effective masses, and confinement energies. For more information on EPAPS, see http://www.aip.org/pubservs/epaps.html.
[24] http://semiconductor.physics.uiowa.edu
[25] R. T. Tung, Phys. Rev. B **45**, 13509 (1992).
[26] S. Nie and S. R. Emory, Science **275**, 1102 (1997).
[27] K. Flensberg, Phys. Rev. Lett. **81**, 184 (1998).
[28] D. Allender, J. Bray, and J. Bardeen, Phys. Rev. B **7**, 1020 (1973).
[29] A. R. Goñi, A. Pinczuk, J. S. Weiner, J. M. Calleja, B. S. Dennis, L. N. Pfeiffer, and K. W. West, Phys. Rev. Lett. **67**, 3298 (1991).